TRAVEL BUBBLE DECISION USING METAPOPULATION EPIDEMIC AND MOBILITY MODEL

Yang LIU[1] and Shinya HANAOKA[2]

[1]Doctor Student, Dept. of Transdisciplinary Science and Engineering, Tokyo Institute of Technology
(12-1, Ookayama 2, Meguro-ku, Tokyo 152-8550, Japan)
E-mail: liu.y.cf@m.titech.ac.jp
[2]Member of JSCE, Professor, Dept. of Transdisciplinary Science and Engineering, Tokyo Institute of Technology
(12-1, Ookayama 2, Meguro-ku, Tokyo 152-8550, Japan)
E-mail: hanaoka.s.aa@m.titech.ac.jp

The COVID-19 pandemic has posed a tremendous impact on transportation and tourism sectors. As vaccines were being administered and lockdowns implemented, owing to the significant social and economic impacts, travel bubbles were proposed as a gradual and intermediate open policy to balance risks and economic recovery. However, the travel bubble framework and associated costs and benefits were not well-established during policy implementation. In this study, we propose a novel travel bubble transportation framework using a metapopulation model, and conduct a cost–benefit analysis for the decision-making process. Our model focuses on the control of both domestic and international long-distance travel inside the bubble, to maximize monetary returns derived from tourism benefits and pandemic costs. A sequential decision problem is proposed to make multiple decisions based on real-time observations. We conduct a case study on travel bubbles in Australia, New Zealand, and Japan to test the model's feasibility. The simulation results show that a controlled intra-bubble transportation can generate positive economic benefits while keeping the epidemic within an acceptable range of control. Our framework can assist policymakers in making informed open decisions by considering multiple attributes during a global pandemic.

Key Words : *COVID-19, travel bubble, metapopulation, transportation, decision-making*

1. INTRODUCTION

After the first documented case of COVID-19 emerged in Wuhan in December 2019, the local outbreak rapidly transformed into a severe worldwide pandemic in just a few months, mainly propelled by international travel[1)]. By April 2020, all travel destinations had imposed restrictions in response to the pandemic[2)], leading to a significant reduction of around one billion international tourist arrivals in 2020 and 2021 compared to that in 2019[3)]. The aviation industry also suffered significantly, with an accumulated loss of $180 billion by the end of 2021[4)]. In addition, the implementation of stringent and prolonged travel restrictions resulted in increased stress and anxiety among the public, adversely affecting the mental health of those impacted[5), 6)].

From past experience, we can infer: (i) lockdowns and travel restrictions are effective in containing the spread of a virus[7), 8)], but tremendously impact the economy and public mental health; (ii) as vaccines are being administered[9)], a gradual and safe reopening process is necessary for economic recovery[10)]; and (iii) be it a complete lockdown or a full opening, both are extreme measures during a global pandemic, necessitating that policymakers adopt intermediate policies to balance risk management and tourism market needs[11)]. To address these issues, the concept of travel bubbles, also referred to as *travel corridors*, *air bridges*, or *corona corridors*[12)], has emerged as a potential solution. A travel bubble, established through bilateral or multilateral agreements, selectively opens borders between specific countries or regions, allowing cross-border travel without mandatory quarantine requirements.

The Baltic travel bubble, announced in May 2020 to ease travel restrictions among Lithuania, Estonia, and Latvia, ended in September 2020 due to an increase in infected cases in[13), 14)]. In July that year, four Canadian provinces established the Atlantic Bubble Agreement, which was suspended in November[15)]. Asia's first travel bubble between Taiwan and Palau

came into effect in April 2021, but had to be discontinued within two months owing to a case spike in Taiwan[16]. In May 2020, the Trans-Tasman bubble, which facilitated travel between Australia and New Zealand, was initially announced in a partial and brief manner; it was later relaunched in April 2021 and remained operational for three months[17]. Other travel bubbles briefly established or temporarily discussed include the New Zealand and Cook Islands travel bubbles[18], Japan's travel bubble with five Asian regions[19], the green lane agreement between Singapore and Malaysia[20], and the Transatlantic air bridge connecting London and New York[21]. Based on this historical context, it is apparent that bubble policies were susceptible to suspension due to unexpected case spikes, resulting in intermittent disruptions to businesses and public concerns.

The study of travel bubble has not been well extended, primarily focusing on survey-base intention analysis, case-specific discussions, and data evidence study. The literature review on the related subjects is listed as follow. Sharun et al. (2020) explored the implications and risks associated with several proposed travel bubbles, and concluded it necessary to establish safe and efficient travel bubbles. They also emphasized on the significance of mathematical modeling in offering valuable insights for devising diverse strategies to ease travel restrictions[12]. Oliu-Barton and Pradelski (2021) highlighted the effectiveness of a Green Zoning strategy in controlling the spread of the virus and mitigating adverse economic and social effects. However, the authors also identified two issues with this approach: potential limitations on civil liberties and challenges of fluctuating restrictions leading to business disruptions and psychological burdens on the public[22]. Dave et al. (2023) developed a quantitative model based on social and public health vulnerabilities to identify low-risk inter-district travel bubbles in India. The discussion on travel bubble policies has been enriched with valuable insights from survey-based studies[23]. For instance, Luo and Lam (2020) emphasized the significance of reducing people's anxiety and fostering a positive risk attitude when implementing tourism bubbles[24]; while Yu et al. (2021) examined individuals' willingness to participate in travel bubbles and identify various positive and negative drivers influencing policymaking[25]. Sun et al. (2022) analyzed flight data from 2019 and 2020 to identify the presence of travel bubbles in certain country pairs. Their findings revealed that some countries maintained higher connectivity with selected destinations than with other countries during the pandemic[26]. Sun et al. (2023) likened the travel bubble policy to a "*tightrope walk*" through a comprehensive discussion. It included various perspectives of the establishment and the maintenance of the travel bubble based on the Trans-Tasmanian case. They pointed out that complete isolation and vaccination were important factors in shaping and reshaping COVID-zero travel bubbles[17].

In this study, we first introduce a Suspectable-Vaccinated-Latent-Infectious-Removed (SVLIR) epidemic model and incorporate it into a metapopulation framework. Metapopulation models have been widely used to estimate epidemic spread, especially concerning the effects of human transportation and mobility[27, 28]. Upon this framework, we formulate a transportation control model for travel bubbles and develop a decision-making process that considers pandemic-related costs and tourism-related benefits during the bubble implementation phase. This study addresses the control of domestic and international long-distance travel, striking a balance between the epidemic cost and economic benefit derived from increased mobility within the bubble. We focus on the vaccine roll-out period, during which there is no exponential growth in cases and there are no stringent COVID-zero requirements in place. Our objective is to obtain an optimal strategy for controlling transportation inside the bubble system. We formulate an optimization problem to maximize financial gains from tourism benefits while effectively managing pandemic-related costs with respect to the limitation of medical capacity. We later extend the optimization problem to a sequential decision problem (SDP) to make real-time decisions based on observations. A stage-aggregated direct lookahead method is provided to solve the SDP, followed by a numerical experiment to test the feasibility of the model. Our model incorporates medical capacity constraints to ensure that epidemic situations remain within feasible limits. This research marks a pioneering endeavor for managing the travel bubble framework and quantifying the associated risks and benefits in the reopening phase during a pandemic. Using the outputs of our model, policymakers can make informed border-open decisions by considering various attributes. It should be noted that although the travel bubble policy has not been successful, its analysis remains important in preparation for future pandemics.

The remainder of this paper is organized as follows. In Section 2, we present a modified metapopulation epidemic model and epidemic variations caused by cross-regional travel and mobility of individuals. Section 3 discusses the development of the travel bubble framework and the optimization problem of transport control. Section 4 presents the simulation results of numerical experiments. Finally, in Section 5, we present the conclusions and propose several directions for future research.

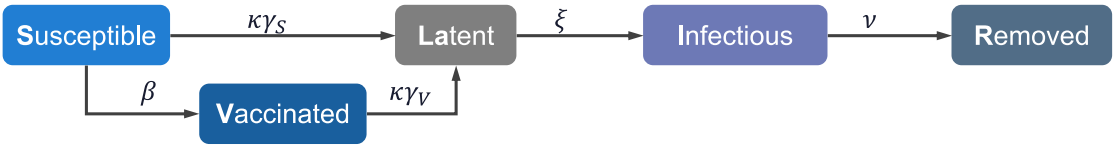


Fig. 1 SVLIR epidemic compartmental structure.

2. METAPOPULATION MODEL

In this section, we introduce the metapopulation epidemic and mobility model. The SVLIR epidemic model is introduced in subsection (1), and the variations in epidemic dynamics caused by long-distance travel and local commuting by individuals are discussed in subsections (2), and (3), respectively.

(1) Epidemic model

In the metapopulation model, a large population is divided into several smaller spatially separated subpopulations. Each of them is located in their respective subpopulation region (hereinafter simply referred to as "region"). Subpopulations are interconnected through the occasional transportation of individuals between them. In each region, disease transmission was formulated using an SVLIR epidemic model[28), 29)]. **Fig. 1** illustrates the compartmental structure of the epidemic model. For region j, the total population is denoted as a constant N_j. This indicates that the population does not change over time. Susceptible individuals can be infected at a rate $\kappa_j\gamma_S$, where κ_j is the contact rate per unit time in region j and γ_S is the disease transmissibility among suspectable individuals; susceptible individuals can also be vaccinated at rate β_j. Vaccinated individuals can be infected at a lower rate at $\kappa_j\gamma_V$. Latent individuals are those already infected, but not yet infectious—and will progress to infectious status at the end of the latency period ξ^{-1}. Infected individuals can infect people who are susceptible or vaccinated and will be moved to the removed phase after ν^{-1}; removed individuals can no longer infect or be infected (including those who are isolated, recovered, or dead). The formulation of the epidemic model system is summarized in equations (1a) – (1e):

$$\Delta S_j/\Delta t = -\kappa_j\gamma_S I_j S_j/N_j - \beta_j S_j, \quad (1b)$$

$$\Delta V_j/\Delta t = \beta_j S_j - \kappa_j\gamma_V I_j V_j/N_j, \quad (1c)$$

$$\Delta L_j/\Delta t = \kappa_j I_j(\gamma_S S_j + \gamma_V V_j)/N_j - \xi L_j, \quad (1d)$$

$$\Delta I_j/\Delta t = \xi L_j - \nu I_j, \quad (1e)$$

$$\Delta R_j/\Delta t = \nu I_j.$$

The dynamics of each epidemic compartment in each region is integrated with the cross-regional mobility of individuals, including long-distance travel and local commuting[28)].

(2) Long-distance travel

We define long-distance travel as air, railway, and cruise ship travel, which are cross-regional modes of travel. Herein, travelers have a certain period of stay in the destination region. The long-distance travel matrix is defined as $\boldsymbol{X}(t)$, where the elements denote the number of long-distance travelers between all origin–destination pairs at time t. We assumed that travel operators precisely forecast the long-distance travel matrix according to the market.

In long-distance transport, compartment variation is caused by individuals traveling from and to different regions. The epidemic dynamics with long-distance travel can be formulated as:

$$N_j^{[m]}(t+1) = N_j^{[m]}(t) + \Delta N_j^{[m]}(t) + \sum_i \left(X_{ij}^{[m]}(t) - X_{ji}^{[m]}(t)\right) \quad (2)$$

where $m \in \{S, V, L, I, R\}$ denotes the epidemic compartment (e.g., $N_j^S(t) = S_j(t)$). $X_{ij}^{[m]}(t)$ is the number of long-distance travelers from i to j with a health state of m at time t, which can be calculated by multiplying the total number of travelers, $X_{ij}(t)$, by the percentage of individuals in the original region who are in health state m, denoted by $p_i^{[m]}(t)$. The formulation of $X_{ij}^{[m]}(t)$ is as follows:

$$X_{ij}^{[m]}(t) = X_{ij}(t)p_i^{[m]}(t) = X_{ij}(t)\frac{N_i^{[m]}(t)}{N_i}. \quad (3)$$

In addition, several studies have revealed evidence of a positive association between the number of travelers visiting a region and the number of infections, as well as the infection growth rate in that region[30), 31)]. In our analysis, we assumed travelers do not change the disease transmissibility (represented by γ_S and γ_V), but do change the local contact rate κ owing to their high mobility. The adjusted contact rate $\hat{\kappa}_j$ is determined as a function of the resident contact rate and the number of inbound travelers:

$$\hat{\kappa}_j = \mathcal{P}\left(\kappa_j, X_j(t)\right), \quad (4)$$

where $X_j(t) = \sum_i X_{ij}(t)$. We divided travelers into two groups: (i) inbound tourists and (ii) residents returning from their trips. Owing to the demands associated with sightseeing and shopping, inbound tourists exhibit a higher daily contact rate than residents

do. To capture this phenomenon, we introduce a coefficient, denoted as η (constant and ≥ 1). It is multiplied by the contact rate of the residents to determine the contact rate of tourists upon their arrival in the destination region. With these assumptions, the adjusted contact rate in region j can be derived as follows:

$$\hat{\kappa}_j = 1/N_j \left[\left(N_j - \alpha_j t_s X_j(t)\right)\kappa_j + \alpha_j t_s X_j(t)\eta\kappa_j\right] = \kappa_j + (\eta - 1)\alpha_j t_s X_j(t)\kappa_j / N_j, \quad (5)$$

where α_j is the fraction of inbound tourists among all travelers arriving in region j (only inbound tourists will have higher mobility and the returning residents from the trip do not increase local mobility), and t_s represents the average duration of tourists' visits to the destination region. Given that the longer tourists stay in the destination region, the greater is the number of tourists in that region, we approximate the total number of tourists in region j at time t by multiplying the daily inbound tourists by the length of their stay, denoted as $\alpha_j t_s X_j(t)$.

(3) Local commuting

We define local commuting as traveling to adjacent regions for school or work with frequent returns. According to Balcan et al. (2010)[28], each compartment population $N_j^{[m]}(t)$ can be divided into two parts: people from region j located in j at time t, denoted by $N_{jj}^{[m]}(t)$; and people from j, located in other regions because of commuting, denoted by $N_{ji}^{[m]}(t)$. We consider σ_{ji} as the commuting rate of residents from region j to adjacent region i, $\sigma_j = \sum_i \sigma_{ji}$, and τ as the return rate; then, the compartment dynamic with local commuting $\bar{N}_j^{[m]}(t)$ is derived as

$$\bar{N}_j^{[m]}(t) = N_{jj}^{[m]}(t) + \sum_i N_{ji}^{[m]}(t) = \frac{N_j^{[m]}(t)}{1+\sigma_j/\tau} + \sum_i \frac{N_j^{[m]}(t)}{1+\sigma_j/\tau}\frac{\sigma_{ji}}{\tau} = c_j^e N_j^{[m]}(t), \quad (6)$$

where $c_j^e = \frac{1}{1+\sigma_j/\tau} + \sum_i \frac{1}{1+\sigma_j/\tau}\frac{\sigma_{ji}}{\tau}$.

The effective infection forces among susceptible and vaccinated individuals are denoted by λ_j^S and λ_j^V, respectively. However, each is also divided into two parts: (i) infection by interaction when commuting in the residence region and (ii) infection by interaction when traveling to adjacent regions. The formulations for the effective infection forces are:

$$\lambda_j^S = \frac{\lambda_{jj}^S}{1+\sigma_j/\tau} + \sum_i \frac{\lambda_{ji}^S \sigma_{ji}/\tau}{1+\sigma_j/\tau}, \quad (7a)$$

$$\lambda_j^V = \frac{\lambda_{jj}^V}{1+\sigma_j/\tau} + \sum_i \frac{\lambda_{ji}^V \sigma_{ji}/\tau}{1+\sigma_j/\tau}, \quad (7b)$$

where $\lambda_{jj}^S = \frac{\hat{\kappa}_j \gamma_S}{N_j}\left[\frac{I_j}{1+\sigma_j/\tau} + \sum_i \frac{I_i}{1+\sigma_i/\tau}\frac{\sigma_{ij}}{\tau}\right]$,
$\lambda_{ji}^S = \frac{\hat{\kappa}_i \gamma_S}{N_i}\left[\frac{I_i}{1+\sigma_i/\tau} + \sum_l \frac{I_l}{1+\sigma_l/\tau}\frac{\sigma_{li}}{\tau}\right]$,
$\lambda_{jj}^V = \frac{\hat{\kappa}_j \gamma_V}{N_j}\left[\frac{I_j}{1+\sigma_j/\tau} + \sum_i \frac{I_i}{1+\sigma_i/\tau}\frac{\sigma_{ij}}{\tau}\right]$ and
$\lambda_{ji}^V = \frac{\hat{\kappa}_i \gamma_V}{N_i}\left[\frac{I_i}{1+\sigma_i/\tau} + \sum_l \frac{I_l}{1+\sigma_l/\tau}\frac{\sigma_{li}}{\tau}\right]$.

3. TRAVEL BUBBLE FORMULATION

In this section, we propose a mathematical formulation of the travel bubble framework with the transportation control variable under the metapopulation model described in subsection (1). Based on this framework, we introduce the optimization problem and SDP in subsections (2) and (3), respectively.

(1) Mathematical formulation

The travel bubble policymaking framework is presented in **Fig. 2**; each subpopulation region comprises three layers of information: (i) the population layer, which determines the local contact rate based on the population size and density, (ii) the mobility layer, which accounts for local commuting and long-distance transport, as discussed in Section 2, and (iii) the epidemic layer, which utilizes the SVLIR model

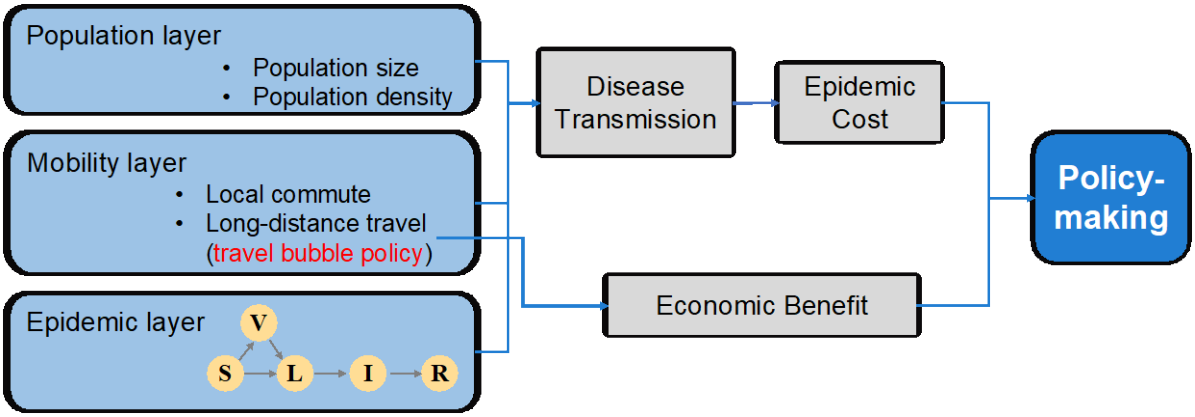


Fig. 2 Travel bubble policy-making framework with the metapopulation model.

to capture the regional epidemic compartment transition. The combination of these layers in all subpopulations determines disease transmission and contributes to the overall epidemic cost. Controlling long-distance travel within a travel bubble offers economic benefits to tourism and other economic activities. The policymaking process considers costs and benefits as determining factors.

In the travel bubble, we suppose there are a total of D countries involved, and isolated from countries other than those, $\mathcal{D} = \{1, 2, \cdots, D\}$ denotes the set of countries. The set of the subpopulation regions in country $d \in \mathcal{D}$ is denoted as $\mathcal{K}_d$, and $\mathcal{K} = \cup_{d=1}^{D} \mathcal{K}_d = \{1, 2, \cdots, K\}$ denotes the set of all subpopulation regions in the travel bubble. $\mathcal{T} = \{1, 2, \cdots, T\}$ is the discretized time of the total studied period, and the minimal time scale is set to be 1 day.

The symmetric connectivity matrix $\boldsymbol{\delta} \in R^{D \times D}$ is defined as the policy variable for country-level transport control. The elements in $\boldsymbol{\delta}$ are defined as

$$\delta_{d_1,d_2} = \delta_{d_2,d_1} \in [0,1], \ \forall d_1, d_2 \in \mathcal{D}. \tag{8}$$

$\delta_{d_1,d_2} = 0$ indicates complete border closure between country d_1 and d_2 if $d_1 \neq d_2$, or strict domestic travel control if $d_1 = d_2$. $\delta_{d_1,d_2} = 1$ indicates a fully open or uncontrolled state for international or domestic travel.

We modify the epidemic model formulated in equations (1a – e) to include travel control policy variables, and obtain the following metapopulation epidemic model system:

$\forall d_1 \in \mathcal{D}, \forall j \in \mathcal{K}_{d_1}$,

$$S_j(t+1) = c_j^e S_j(t) - (\lambda_j^S + \beta_j) S_j(t) + \sum_{d_2 \in \mathcal{D}} \left\{ \delta_{d_1,d_2} \cdot \sum_{k \in \mathcal{K}_{d_2}} (X_{kj}^S - X_{jk}^S) \right\}, \tag{9a}$$

$$V_j(t+1) = c_j^e V_j(t) + \beta_j S_j(t) - \lambda_j^V V_j(t) + \sum_{d_2 \in \mathcal{D}} \left\{ \delta_{d_1,d_2} \cdot \sum_{k \in \mathcal{K}_{d_2}} (X_{kj}^V - X_{jk}^V) \right\}, \tag{9b}$$

$$L_j(t+1) = c_j^e L_j(t) + \lambda_j^S S_j(t) + \lambda_j^V V_j(t) - \xi L_j(t) + \sum_{d_2 \in \mathcal{D}} \left\{ \delta_{d_1,d_2} \cdot \sum_{k \in \mathcal{K}_{d_2}} (X_{kj}^L - X_{jk}^L) \right\}, \tag{9c}$$

$$I_j^a(t+1) = c_j^e \cdot I_j(t) + \xi L_j(t) - \nu I_j(t) + \sum_{d_2 \in \mathcal{D}} \left\{ \delta_{d_1,d_2} \cdot \sum_{k \in \mathcal{K}_{d_2}} (X_{kj}^I - X_{jk}^I) \right\}, \tag{9d}$$

$$R_j(t+1) = c_j^e \cdot R_j(t) + \nu I_j(t) + \sum_{d_2 \in \mathcal{D}} \left\{ \delta_{d_1,d_2} \cdot \sum_{k \in \mathcal{K}_{d_2}} (X_{kj}^R - X_{jk}^R) \right\}. \tag{9e}$$

(2) Static travel bubble decision model

We consider a system-optimal strategy in our travel bubble decision-making process. The strategy helps calculate the overall benefit and cost for all countries involved in the bubble system. The benefit indicates the tourism-added contributed by domestic and international tourists[32], whereas the cost indicates social and individual losses from infection and the cost of vaccination. The optimization problem is formulated as follows:

$$\max_{\boldsymbol{\delta}} \sum_{t \in \mathcal{T}} \sum_{d_1, d_2 \in \mathcal{D}} \sum_{i \in \mathcal{K}_{d_1}, j \in \mathcal{K}_{d_2}} \delta_{d_1,d_2} \alpha_j w_{ij} X_{ij}(t) - \sum_{t \in \mathcal{T}} \sum_{d \in \mathcal{D}} \sum_{j \in \mathcal{K}_d} \left\{ c_j^I \left(\frac{I_j(t)}{P_j^{pop}} \right)^2 + c_j^V S_j(t) \beta_j \right\} \tag{10a}$$

$$\text{s.t. } I_j(t) < g_j, \qquad \forall j \in \mathcal{K}, \forall t \in \mathcal{T}, \tag{10b}$$

$$\delta_{d_1,d_2} \in [0,1], \qquad \forall d_1, d_2 \in \mathcal{D}_2, \tag{10c}$$

$$\text{Eq. 9(a) – 9(e)} \qquad \forall d_1 \in \mathcal{D}, \forall j \in \mathcal{K}_{d_1}, \forall t \in \mathcal{T}.$$

Here, w_{ij} $(i, j \in \mathcal{K})$ denotes the average economic value to the destination region of a tourist traveling from region i to region j; c_j^I is the coefficient of infection cost in region j, including the cost of medical care, opportunity loss of infected individuals, and emotional loss. We adopt a quadratic formulation[33), 34)] of active infected case count per 1000 population ($P_j^{pop} = N_j/1{,}000$). c_j^V is the government cost for each fully vaccinated individual (total 3 doses per person) in region j. Finally, g_j $(j \in \mathcal{K})$ denotes the target level of infection control owing to the limitation of medical resources.

In real-world cases, the policies are discrete rather than continuous, such that we define $\mathcal{A}$ as the set of all feasible policies and each policy subset $\pi^a = \{\delta_{d_1,d_2}^a \,|d_1, d_2 \in D, \delta_{d_1,d_2}^a \in [0,1]\} \subseteq \mathcal{A}$. The static travel bubble decision model can be solved through a direct policy search among finite choices.

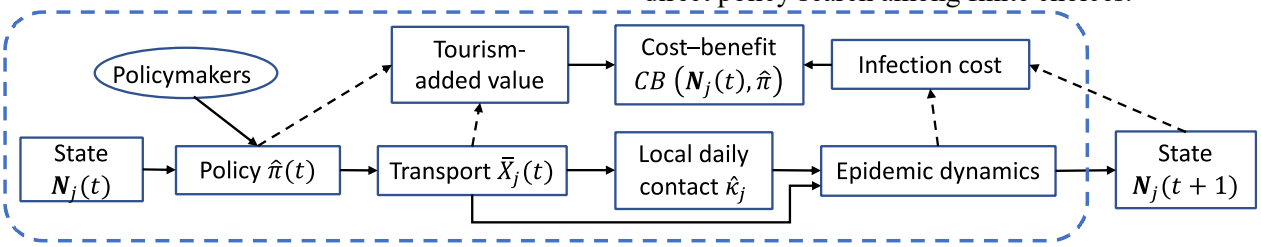


Fig. 3 Decision-making process at time t.

Algorithm 1: Stage-aggregation approximated DLA

Input: discrete policy set $\mathcal{A}$, decision point set $\mathcal{T}_D = \{t_0^{dp}, \cdots, t_B^{dp}\} \subset \mathcal{T}$, cost–benefit function $CB(\cdot)$, initial epidemic condition $\boldsymbol{N}(0)$, transport data $X(t)$, other epidemic and transport parameters.

for $b = 0, \cdots, B$ **do**
  $\boldsymbol{N}_0 = \boldsymbol{N}(t_b^{dp} - 1)$
  $\widehat{CB}_b \leftarrow$ sufficient small number
  for $a = 1, \cdots, A$ **do**
    calculate $CB_b^a = \int_{t=t_b^{dp}}^{T} CB\big((\boldsymbol{N}(t), \pi^a)\big)dt$
    calculate $\boldsymbol{N}_b^a(t)$ with $(\pi^a, \boldsymbol{N}_0)$ for $t = t_b^{dp}, \cdots, T$
    if $CB_b^a > \widehat{CB}_b$ **and** $I_{b,k}^a(t) < g_k$ $(\forall k \in \mathcal{K}, \forall t \in \{t_b^{dp}, \cdots, T\})$ **do**
      $\widehat{CB}_b = CB_b^a$
      $\hat{\pi}_b = \pi^a$
      $\widehat{\boldsymbol{N}}_b(t) = \boldsymbol{N}_b^a(t)$ for $t = t_b^{dp} \cdots, T$

Result: optimal policy $\{\hat{\pi}_1, \hat{\pi}_2, \cdots, \hat{\pi}_B\}$, cost prediction $\{\widehat{CB}_1, \widehat{CB}_2, \cdots, \widehat{CB}_B\}$, epidemic compartment distribution $\{\widehat{\boldsymbol{N}}_b(t_b^{dp}), \cdots, \widehat{\boldsymbol{N}}_b(t_{b+1}^{dp} - 1)\}_{b=0}^{B}$.

(3) Dynamic travel bubble decision model

Based on the static travel bubble decision model, we develop an SDP to enable policymakers to revise their control policies based on prevailing circumstances. Suppose $\mathcal{T}_D = \{t_0^{dp}, \cdots, t_B^{dp}\} \subset \mathcal{T}$ is the set of all decision time points where policymakers need to make a new policy. To reduce the policy switch cost, we assume that a policy at the period of $\{t_b^{dp} + 1, \cdots, t_{b+1}^{dp} - 1\}$ $(b \in \{0, 1, \cdots B\})$ stays the same with the policy made at t_b^{dp}. The control policy is implemented through the decision-making process shown in **Fig. 3**. The cost–benefit CB as a function at time t_b^{dp} with policy π^a in the process is denoted as:

$$CB\left(\boldsymbol{N}(t_b^{dp}), \pi^a\right) = \sum_{d_1, d_2 \in \mathcal{D}} \sum_{i \in \mathcal{K}_{d_1}, j \in \mathcal{K}_{d_2}} \delta_{d_1, d_2}^a \alpha_j w_{ij} X_{ij}(t_b^{dp}) - \sum_{d \in \mathcal{D}} \sum_{j \in \mathcal{K}_d} \left\{ c_j^I \left(\frac{I_j(t)}{P_j^{pop}} \right)^2 + c_j^V S_j(t) \beta_j \right\} \quad (11)$$

where $\boldsymbol{N}(t)$ is the column vector used to store the epidemic data for all the regions in $\mathcal{K}$ at time t. Policymakers determine a policy $\hat{\pi}(t)$ to maximize the long-term cost–benefit function through an SDP:

$$\hat{\pi}(t) = \underset{\pi \in \mathcal{A}}{\operatorname{argmax}} \left\{ CB\left(\boldsymbol{N}(t), \pi\right) + \max_{\pi^{t'} \in \mathcal{A}} \int_{t'=t+1}^{T} CB\left(\left(\boldsymbol{N}(t'), \pi^{t'}\right)\right) dt' \right\} \quad (12)$$

We use the stage-aggregation approximated direct lookahead (DLA) method developed by Powell (2021)[34] to solve the SDP in equation (12). This method is summarized in Algorithm 1. Given that the static control problem in subsection 4(2) can be considered as an SDP with only one decision-making point at $t = 0$, the static and dynamic problems can both be solved using **Algorithm 1**.

4. NUMERICAL RESULTS

To depict travel bubble control policies within our mathematical framework, we perform a numerical experiment involving three countries: Japan (JP), Australia (AU), and New Zealand (NZ). All the three countries are well connected in the tourism market. AU is the 1st and the 7th largest tourism market resource for NZ and JP; NZ is the 2nd largest tourism market resource for AU; and JP is the 5th and 6th largest tourism market source for AU and NZ, respectively[36), 37), 38)]. **Fig. 4** presents a summary of passenger data within and between the three countries during the latter half of 2019 and 2020. The reduction in domestic air transport in 2020 from 2019 was over 70%, and for international air transport, over 95%. Therefore, there was a potential need for these three countries to establish travel bubbles. We divide JP, AU, and NZ into 8, 8, and 16 subpopulation regions,

respectively, based on their administrative divisions. The population and population density information for each region are obtained from official government websites[39), 40), 41)].

In our assumption, the travel bubble policy is subject to discussion only when the infection case remains below a certain threshold, specifically 0.05 active infectious cases per 1,000 people. In the simulation, the initial infection case count is set based on this assumption. Other relevant pandemic data are collected from the WHO Coronavirus Dashboard[42)]. Our experiment period starts from July 1, 2020, and spans a total period of 180 days. Owing to data limitations, this simulation exclude long-distance travel by railway and cruise ships, focusing solely on air transport. The flight data is sourced from OAG[43)], and the passenger data is calculated by multiplying the seat count with an approximate annual passenger load factor[44), 45)]. Without loss of generality, we use these data as the long-distance OD travel matrix $\boldsymbol{X}$ by ignoring transit flights. We assume that the infection

Table 1 Parametric values used in the numerical experiment.

Parameters	Description	Value	Reference
γ_S	Infection rate of unvaccinated individuals	0.007	Liu and Ding, 2022[51)]
γ_v	Infection rate of vaccinated individuals	0.0002	Liu and Ding, 2022[51)]
	Vaccine roll-out rate in JP	0.0021	WHO, 2023[42)]
β	Vaccine roll-out rate in AU	0.0021	WHO, 2023[42)]
	Vaccine roll-out rate in NZ	0.0022	Health New Zealand, 2023[52)]
ξ^{-1}	Latent period	5.5 (d^{-1})	Xin et al., 2022[53)]
ν^{-1}	Infectious period	7 (d^{-1})	MHLW, 2022[39)]
τ^{-1}	Return rate	3 (d^{-1})	Balcan et al., 2010[28)]
c_V	Government cost for a fully vaccinated individual	0.4 (K$)	Mainichi Japan, 2022[54)]
t_s	Average period of tourists' stay at the destination	6	-
η	Tourist mobility coefficient	5	-

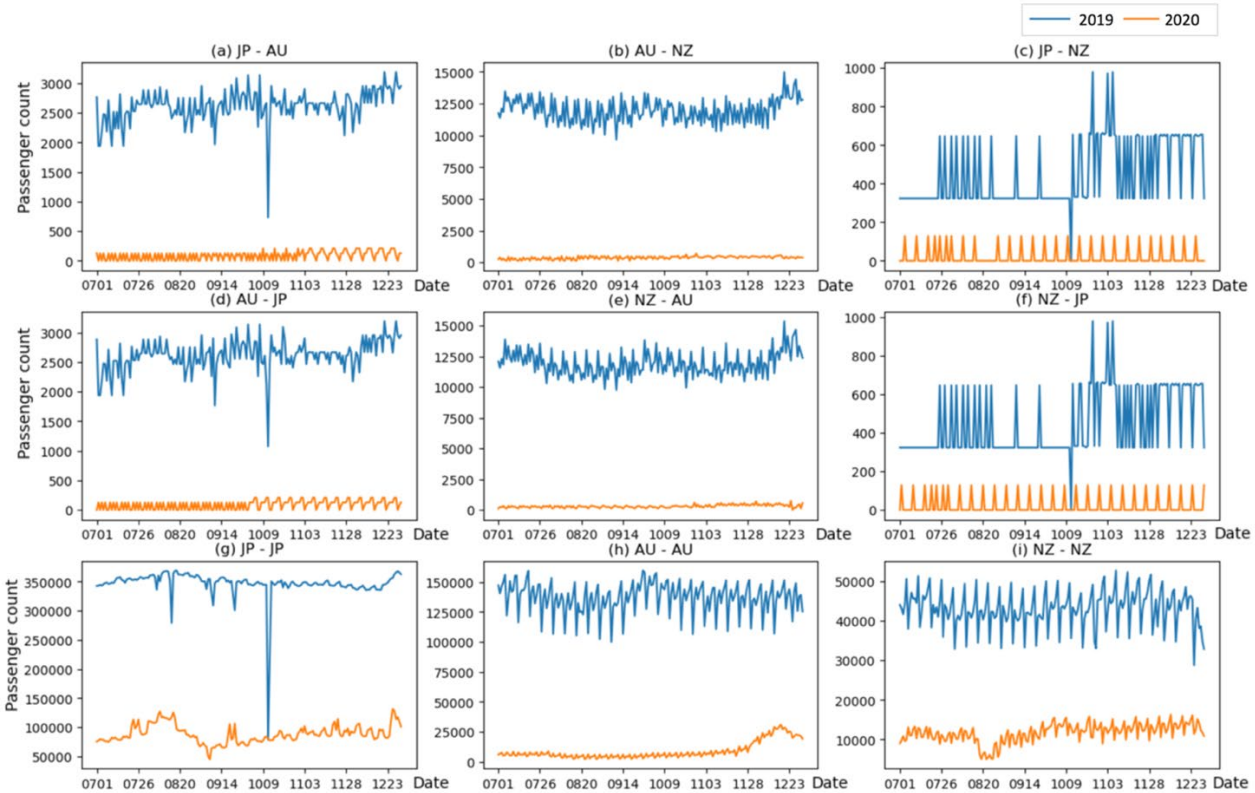


Fig. 4 International and domestic air-travel passenger data in 2019 and 2020 in JP, AU, and NZ.

cost coefficient is $c_j^I = 1 \times P_j^{pop}$ (K$), as estimated from the parameters provided by Wang et al. (2019)[46] and Rocha-Filho et al. (2022)[47]. Commuting rates in JP, AU, and NZ are obtained from Adachi et al. (2020)[48], Australia Bureau of Statistics (2008)[48], and Stats NZ (2018)[49], respectively. The other specific parameters used in the simulation are listed in **Table 1**.

The regional infection target is directly linked to healthcare capacity, specifically the availability of hospital beds for in-patient care. In this simulation, we assume that a maximum of 50% beds are allocated to cater to approximately 53% of the infected individuals[39]. Healthcare capacity data is obtained from the MHLW (2022)[39], Statista (2022)[55], and Wikipedia (2023)[56].

The discrete policies are set as:

$$\delta_{d_1,\,d_2} \in \begin{cases} \{0,\ 0.5,\ 1\}, & \text{if } d_1 \neq d_2 \\ \{0.5,\ 1\}, & \text{if } d_1 = d_2 \end{cases}, d_1,\ d_2 \in \mathcal{D}, \quad (13)$$

which indicates three options for international travel: completely closed ($\delta = 0$), half open ($\delta = 0.5$), and fully open ($\delta = 1$); and two options for domestic travel: half open ($\delta = 0.5$) and fully open ($\delta = 1$).

We explore three scenarios in our experiment: dynamic border open (DBO), dynamic border close (DBC), and static border open (SBO). The DBO and DBC scenarios are the sequential decision problems described in subsection 3(3), with transport control policies renewed every 30 days ($\mathcal{T}_D = \{0,\ 30,\ 60,\ 90,\ 120,\ 150\}$). The SBO scenario is the static optimization problem described in subsection 3(2). The DBO and SBO scenarios have a border-open option with the policy set expressed in equation (13). The DBC scenario considers only domestic transport, where international transport is unequivocally constrained to a value of 0, and domestic control has two available options: $\{0.5,\ 1\}$.

The simulation generates the optimal static control pattern in the SBO scenario:

$$\hat{\boldsymbol{\delta}} = \begin{bmatrix} 0.5 & 1 & 0 \\ 1 & 1 & 0.5 \\ 0 & 0.5 & 0.5 \end{bmatrix},$$

where subscripts 1, 2, and 3 correspond to JP, AU, and NZ, respectively. The results indicate that domestic transport within AU is uncontrolled, implying that there are no restrictions or regulations imposed on domestic long-distance travel within the country. By contrast, JP and NZ need to reduce their domestic transport ($\delta = 0.5$) to slow down infection. Regarding international travel, there is a fully open tourism connection between JP and AU, implying a complete recovery of the tourism market to its pre-pandemic level. However, the borders are completely closed for the JP–NZ pair, and only partially open between AU and NZ.

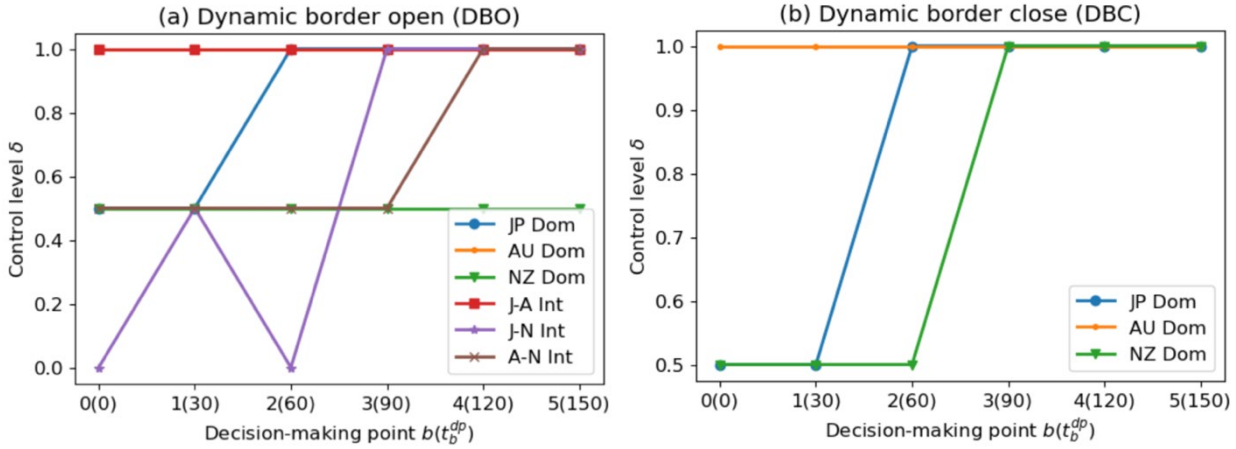


Fig. 5 Control-level dynamics at each decision point in the DBO and DBC scenarios.

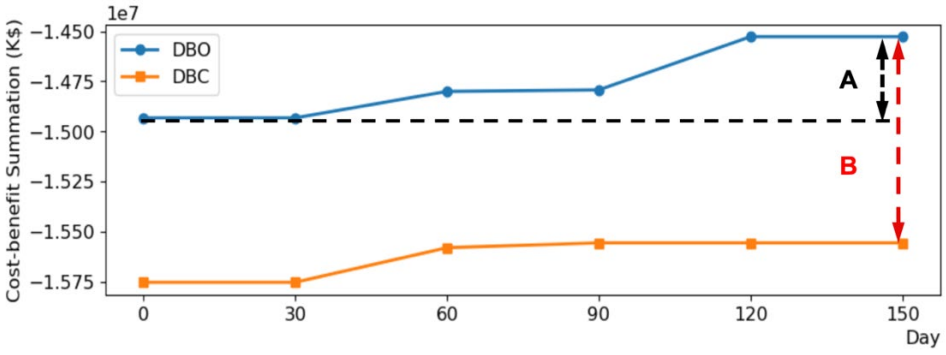


Fig. 6 Overall cost–benefit summation at each decision-making point.

In both dynamic scenarios, **Fig. 5** illustrates the control level for each international and domestic transportation mode at each decision time point. Based on these results, we can observe that in the absence of a travel bubble, both JP and NZ require stringent domestic control measures when vaccinations are insufficient. Specifically, JP reaches an uncontrolled domestic transportation state at decision point $b = 2$, whereas NZ reaches the same at $b = 3$. However, when a bubble is established to facilitate cross-border travel, NZ under the DBO scenario could cautiously open up international tourism while maintaining fluctuating controls. Despite this, domestic travel is kept at a controlled level ($\delta = 0.5$).

The monetary outcomes of the dynamic control strategy, with and without the open-border option, are shown in **Fig. 6**. The dynamic control strategy evidently generates a consistent monetary improvement following each decision point. The strategy also provides an approximate benefit improvement of 405.4 million dollars over the static control measures (gap A in **Fig. 6**). Additionally, the adoption of a border-opening policy, as opposed to border closure, yields a benefit improvement of approximately 1,029 million dollars for the entire bubble system (gap B).

The advantages of implementing dynamic control of border openness over border closure are illustrated in **Fig. 7** for each country. The results indicate that participating in the travel bubble and opening borders are advantageous for all countries involved, although the benefits are not evenly distributed. In this case, AU has the highest benefit, followed by NZ and JP, in descending order. It is worth noting that the optimal system solution may not align with the optimal outcomes for each country. For instance, the connection pattern established at $t_b^{dp} = 30$ generates the highest monetary outcome for JP, compared with the connection patterns made at other decision-making points (**Fig. 7(a)**).

Fig. 8 illustrates the active and cumulative infection trends for each country under the three scenarios. The impact of opening borders within the travel bubble is readily evident in AU, with the cumulative infection increasing by 14.3% compared with that for closed borders. However, the increase is only 0.3% in JP. This is attributed to its substantially larger population than that of AU and NZ. As NZ has different domestic control policies in the DBO and DBC scenarios, the cumulative infection rate without an open border is 9.5% higher. We can deduce that the unchanged domestic control in New Zealand in the DBO scenario is due to the fact that international tourists can generate greater economic benefits than domestic tourists while involving fewer travelers. As

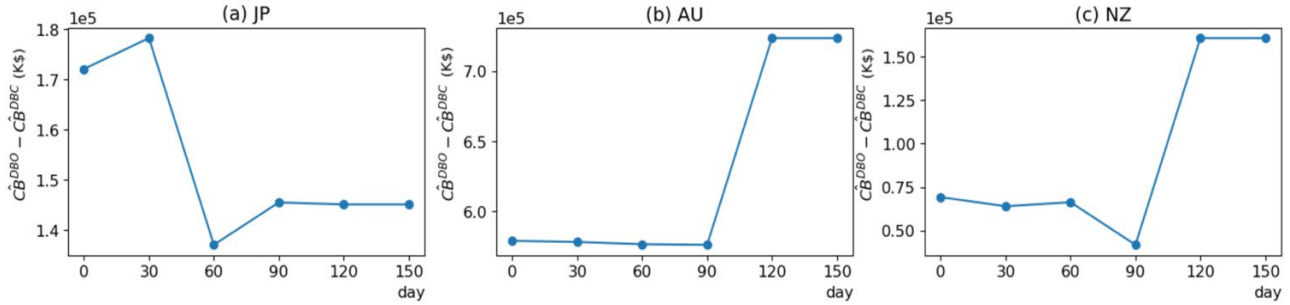


Fig. 7 Benefit of dynamic control of border-opening over border closure for each country.

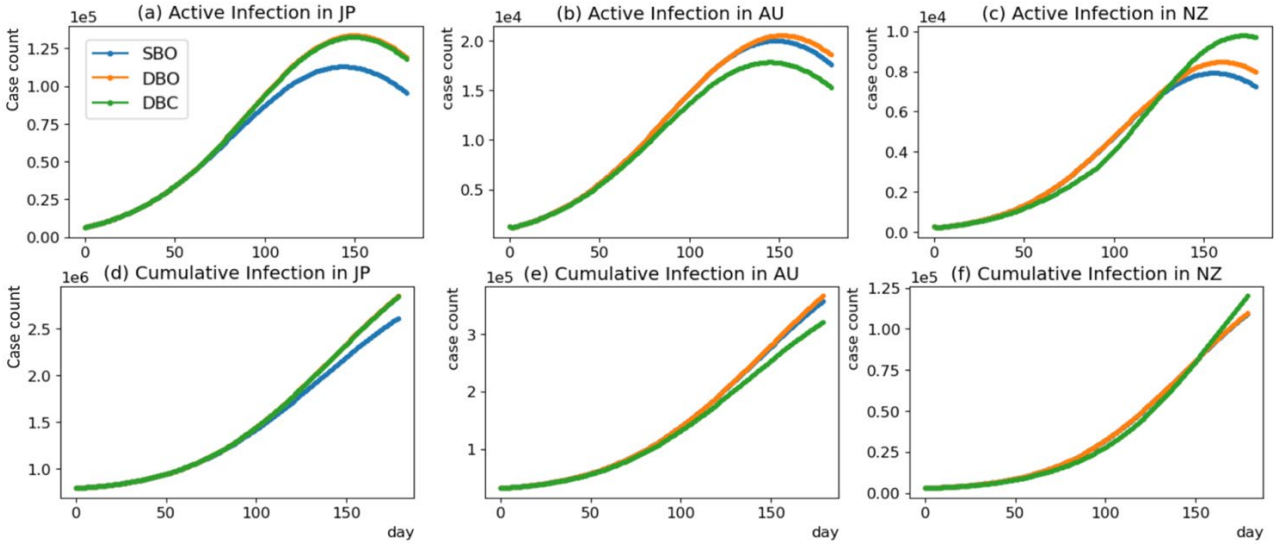


Fig. 8 Infection case trend with different control patterns in JP, AU, and NZ.

is evident in **Fig. 6**, the cost–benefit summation in the DBC scenario shows a relatively smaller increase from $t = 60$ to $t = 90$ owing to the loosening of NZ's domestic control. In contrast, the cost–benefit summation in the DBO scenario experiences a much more significant rise, from $t = 90$ to $t = 120$. This is attributed to the opening of more international travel between NZ and AU, specifically from 0.5 to 1.

Our findings suggest that NZ exhibits certain vulnerabilities in this travel bubble, arising from two factors. Firstly, the international travel connections of NZ–AU and NZ–JP undergo fluctuating controls (**Fig. 5(a)**), necessitating frequent adjustments to NZ's transportation policy due to pandemic control. Secondly, the domestic transportation in NZ remains controlled when the border is opened to JP and AU. This indicates a risk of exceeding the infection target when facing simultaneous demand from domestic and international travel. The dynamic nature of international travel connections requires policymakers in NZ to remain vigilant and adaptive to the evolving global travel landscape. The travel bubble presents an opportunity for economic recovery. Nevertheless, the fluidity of international travel demands a constant reassessment of transportation policies to manage potential public health risks effectively.

The stability of domestic transportation control within AU is maintained in both, the open-border and closed-border scenarios. This is attributed to the robust medical-care capacity that effectively contains infections within each region. For the AU case, the influx of international tourists from NZ and JP leads to an increase in infection cases across all regions in AU. Nevertheless, the advantages of participating in this travel bubble primarily manifest within AU, as highlighted in **Fig. 7(b)**. Additionally, for all three countries. the volume of domestic travel far surpasses that of international travel, making domestic transport a critical factor in shaping the overall epidemical impact of the travel bubble. The infection case trends in JP and NZ further highlight the importance of domestic control measures (**Fig. 8**). When the domestic control measures are raised from 0.5 to 1, noticeable inflection points can be observed in the curves representing the dynamic border-opening and closure scenarios. These inflection points represent significant shifts in the infection case trajectory, and underline the noticeable influence of domestic transport management on a country's epidemiological situation.

In our model, we do not explicitly address the transitive effects. Nonetheless, these effects play a crucial role in influencing the stability of a travel bubble and could potentially lead to its collapse[57]. As demonstrated in our experiment, if the JP–NZ travel corridor is closed, individuals can still travel between JP and NZ via AU. In such scenarios, our framework treats such travels as two distinct segments: one between NZ and AU, and another between JP and AU. Importantly, closing the JP–NZ pair does not lead to an increase in flights between JP–AU or NZ–AU. If JP, AU, and NZ successfully mitigate disease transmission in this context, the travel bubble would remain viable.

5. CONCLUSION

This study introduces a novel mathematical structure for travel bubbles. Our research is driven by the significant economic impact of travel restrictions during the COVID-19 pandemic and the complexities of decision-making regarding border reopening. The proposed framework aims to aid policymakers in making informed decisions regarding the control of domestic and international long-distance travel. The primary objective of the framework is to optimize long-term benefits from the tourism market, while mitigating the risk of increased infection caused by the movement of individuals. These findings underscore the dynamic nature of international travel connections, necessitating a vigilant and adaptive approach from policymakers. Within the travel bubble framework, a flexible and proactive stance is thus imperative to effectively manage the challenges posed by international travel. By embracing our approach, policymakers can strike a balance between revitalizing the tourism industry and safeguarding public health.

Our study uses a metapopulation model to partition countries into smaller subpopulation regions. This enables us to estimate the direct impact of international as well as domestic transport on pandemic control. We develop an optimization problem and an SDP to determine the best control policy for the travel bubble system to obtain the maximum monetary return. While the overall system may benefit from the travel bubble, the specific vulnerabilities and unbalanced benefit distribution experienced by certain countries highlight the need for tailored and adaptive transportation policies.

By adjusting the model parameters or epidemic compartments, our research framework can be broadly applied to other pandemics. Besides providing guidance on establishing travel bubbles after epidemic lockdowns, the output of our model can also facilitate future assessments of employing the travel bubble approach directly at the onset of a pandemic. Furthermore, this analysis reveals the dynamics of connectivity, traffic patterns, and overall resilience. This enables a comprehensive understanding of how

transport networks adapt and evolve in response to a global pandemic.

This study can be extended to a broad range of decision-making problems. Although it considered the vaccination rate as an irrelevant factor for transportation control, it is worth noting that higher vaccination rates can contribute to a reduction in infection counts and subsequently increase the likelihood of opening borders to more tourists. In addition, the geographical distribution of vaccination resources can have a significant role in influencing border reopening. Furthermore, the incorporation of additional policies, such as pre-departure screening, contact tracing, and social distancing, can be explored in the model to assess the effectiveness of various policy combinations. This extension will allow a more comprehensive evaluation of the impact and efficacy of different strategies in mitigating the spread of infectious diseases.

The current research can be further improved as follows: (i) although our model generates the optimal output for the bubble system, it does not guarantee an optimal outcome for each country involved; (ii) our simulation overlooks the influence of transit passengers and the distinction between international and domestic travelers; and (iii) our model encounters a challenge known as the curse of dimensionality, which suggests that as the number of countries involved in the decision-making process increases, it becomes increasingly difficult to identify an optimal solution. Future research should focus on adjusting objectives, collecting ample data, and developing efficient algorithms to enhance the accuracy and comprehensiveness of the aforementioned aspects.

ACKNOWLEDGMENTS: Authors are greatful for the financial support of the Japan Science and Technology Agency, the establishment of university fellowships towards the creation of science technology innovation, Grant Number JPMJFS2112.

REFERENCES

1) Sun, X., Wandelt, S., & Zhang, A. : On the degree of synchronization between air transport connectivity and COVID-19 cases at worldwide level. *Transport Policy*, 105, 115–123, 2021.
2) UNWTO : New data shows impact of COVID-19 on tourism as UNWTO calls for responsible restart of the sector. https://www.unwto.org/news/new-data-shows-impact-of-covid-19-on-tourism. 2020. (Accessed on June 30, 2023)
3) UNWTO. Tourism Recovery Gains Momentum as Restrictions Ease and Confidence Returns. https://www.unwto.org/news/tourism-recovery-gains-momentum-as-restrictions-ease-and-confidence-returns. 2022. (Accessed on June 30, 2023)
4) UNWTO. International Tourism and COVID-19. https://www.unwto.org/tourism-data/international-tourism-and-covid-19. 2022. (Accessed on June 30, 2023)
5) IATA. Annual review 2021. https://www.iata.org/contentassets/c81222d96c9a4e0bb4ff6ced0126f0bb/iata-annual-review-2021.pdf. 2021. (Accessed on June 29, 2023)
6) Terry, P. C., Parsons-Smith, R. L., & Terry, V. R. : Mood responses associated with COVID-19 restrictions. *Frontiers in Psychology*, 11, 589598, 2020.
7) Chinazzi, M., Davis, J. T., Ajelli, M., Gioannini, C., Litvinova, M., Merler, S., Pinotti, A. P., Mu, K., Rossi, L., Sun, K., Viboud, C., Xiong, X., Yu, H., Halloran, M. E., Longini JR, I. M., & Vespignani, A. : The effect of travel restrictions on the spread of the 2019 novel coronavirus (COVID-19) outbreak. *Science*, 368(6489), 395–400, 2020.
8) Murano, Y., Ueno, R., Shi, S., Kawashima, T., Tanoue, Y., Tanaka, S., Nomura, S., Shoji, H., Shimizu, T., Nguyen, H., Miyata, H., Gilmour, S., & Yoneoka, D. : Impact of domestic travel restrictions on transmission of COVID-19 infection using public transportation network approach. *Scientific Reports*, 11(1), 1–9, 2021.
9) Ndwandwe, D., & Wiysonge, C. S. : COVID-19 vaccines. Current Opinion in Immunology, 71, 111–116, 2021.
10) Dube, K., Nhamo, G., & Chikodzi, D. : COVID-19 pandemic and prospects for recovery of the global aviation industry. *Journal of Air Transport Management*, 92, 102022, 2021.
11) Altiparmakis, A., Bojar, A., Brouard, S., Foucault, M., Kriesi, H., & Nadeau, R. : Pandemic politics: policy evaluations of government responses to COVID-19. *West European Politics*, 44(5-6), 1159–1179, 2021.
12) Sharun, K., Tiwari, R., Natesan, S., Yatoo, M. I., Malik, Y. S., & Dhama, K. : International travel during the COVID-19 pandemic: implications and risks associated with 'travel bubbles'. *Journal of Travel Medicine*, 27(8), taaa184, 2020.
13) Webb, E., Winkelmann, J., Scarpetti, G., Behmane, D., Habicht, T., Kahur, K., Kasekamp, K., Köhler, K., Miščikienė, L., Misins, J., Reinap, M., Slapšinskaitė-Dackevičienė, A., Võrk, A., & Karanikolos, M. : Lessons learned from the Baltic countries' response to the first wave of COVID-19. *Health Policy*, 126(5), 438–445, 2022.
14) Reuters, : Baltics open Europe's first pandemic 'travel bubble' as curbs ease. https://www.reuters.com/article/us-health-coronavirus-baltic-idUSKBN22Q3KM. 2020. (Accessed on June 30, 2023)
15) Grant, T. : As COVID-19 cases rise, N.L. and P.E.I. exit Atlantic bubble for at least 2 weeks. https://www.cbc.ca/news/canada/nova-scotia/atlantic-bubble-burst-1.5812454. 2020. (Accessed on June 29, 2023)
16) ABC News : Palau's travel bubble popped by Taiwan's COVID-19 spike. https://www.abc.net.au/pacific/programs/pacificbeat/palau-tourism-bubble-burst-taiwan-rising-covid-19/13353754. 2021. (Accessed on June 29, 2023)
17) Sun, X., Wandelt, S., & Zhang, A. : Why are COVID-19 travel bubbles a tightrope walk? An investigation based on the Trans-Tasmanian case. *Communications in Transportation Research*, 3, 100089, 2023.
18) Ardern, J. : *NZ Cook Islands travel bubble significant step in COVID-19 recovery*. https://www.beehive.govt.nz/release/nz-cook-islands-travel-bubble-significant-step-covid-19-recovery. 2021. (Accessed on June 29, 2023)
19) Furutani, K. : Japan has confirmed its travel bubble with five Asian regions – here are the entry rules. https://www.timeout.com/tokyo/news/japan-has-confirmed-its-travel-bubble-with-five-asian-regions-here-are-the-entry-rules-091420. 2020. (Accessed on June 29, 2023)
20) Lim, J. & Kheng, K.S. : There's a pilot for the Asian travel bubble. Here is how to make it work, 2020. https://www.straitstimes.com/opinion/theres-a-pilot-for-

the-asean-travel-bubble-here-is-how-to-make-it-work. 2020. (Accessed on June 29, 2023)
21) Dailymail : US and UK officials begin talks over a transatlantic “air bridge” to allow travel between NYC and London without 14-day quarantine in a bid to boost business and tourism in time for winter. https://www.dailymail.co.uk/news/article-8668373/Officials-begin-talks-transatlantic-air-bridge-allow-travel-NYC-London.html. 2020. (Accessed on June 29, 2023)
22) Oliu-Barton, M., & Pradelski, B. S. : Green zoning: An effective policy tool to tackle the Covid-19 pandemic. *Health Policy*, 125(8), 981–986, 2021.
23) Dave, R., Choudhari, T., Maji, A., & Bhatia, U. : Quantitative framework for establishing low-risk inter-district travel corridors during COVID-19. *Transportation Research Record*, 2677(4), 335–349, 2023.
24) Luo, J. M., & Lam, C. F. : Travel anxiety, risk attitude and travel intentions towards “travel bubble” destinations in Hong Kong: Effect of the fear of COVID-19. *International Journal of Environmental Research and Public Health*, 17(21), 7859, 2020.
25) Yu, J. H., Lin, H. H., Lo, Y. C., Tseng, K. C., & Hsu, C. H. : Is the travel bubble under COVID-19 a feasible idea or not? International *Journal of Environmental Research and Public Health*, 18(11), 5717, 2021.
26) Sun, X., Wandelt, S., & Zhang, A. : Travel bubbles in air transportation: Myth or reality? *Aerospace*, 9(1), 38, 2022.
27) Colizza, V., & Vespignani, A. : Epidemic modeling in metapopulation systems with heterogeneous coupling pattern: Theory and simulations. *Journal of Theoretical Biology*, 251(3), 450–467, 2008.
28) Balcan, D., Gonçalves, B., Hu, H., Ramasco, J. J., Colizza, V., & Vespignani, A. : Modeling the spatial spread of infectious diseases: The Global Epidemic and Mobility computational model. *Journal of Computational Science*, 1(3), 132–145, 2010.
29) Liu, X., Takeuchi, Y., & Iwami, S. : SVIR epidemic models with vaccination strategies. *Journal of Theoretical biology*, 253(1), 1–11, 2008.
30) Skórka, P., Grzywacz, B., Moroń, D., & Lenda, M. : The macroecology of the COVID-19 pandemic in the Anthropocene. *PLOS ONE*, 15(7), e0236856, 2020.
31) Moosa, I. A., & Khatatbeh, I. N. : International tourist arrivals as a determinant of the severity of COVID-19: International cross-sectional evidence. *Journal of Policy Research in Tourism, Leisure and Events*, 13(3), 419–434, 2021.
32) Oxford Economics : *Travel & Tourism Economic Impact Research: Methodology*. WTTC, 2020.
33) Wang, X., Peng, H., Shi, B., Jiang, D., Zhang, S., & Chen, B. : Optimal vaccination strategy of a constrained time-varying SEIR epidemic model. *Communications in Nonlinear Science and Numerical Simulation*, 67, 37–48, 2019.
34) Mallela, A., Lenhart, S., & Vaidya, N. K. : HIV–TB co-infection treatment: Modeling and optimal control theory perspectives. *Journal of Computational and Applied Mathematics*, 307, 143–161, 2016.
35) Powell, W. B. : *Reinforcement learning and stochastic optimization.* John Wiley & Sons, 2021.
36) Stats NZ : Tourism satellite account: 2019. https://www.stats.govt.nz/information-releases/tourism-satellite-account-2019. 2019. (Accessed on June 30, 2023)
37) Tourism Research Australia : Tourism forecasts. https://www.destinationnsw.com.au/wp-content/uploads/2019/09/tourism-research-australia-tourism-forecast-report-2019.pdf. 2019. (Accessed on June 30, 2023)
38) Japan Tourism Agency : White paper on tourism in Japan, 2022. https://www.mlit.go.jp/kankocho/en/siryou/content/001583966.pdf. 2022. (Accessed on June 29, 2023)
39) MHLW, : Handbook of Health and Welfare Statistics 2022. https://www.mhlw.go.jp/english/database/db-hh/2-2.html. 2022. (Accessed on June 30, 2023)
40) Australia Bureau of Statistics : National, state and territory population. https://www.abs.gov.au/statistics/people/population/national-state-and-territory-population/latest-release. 2022. (Accessed on June 29, 2023)
41) Stats NZ : Subnational population estimates (RC, SA2), by age and sex, at 30 June 1996-2022 (2022 boundaries*).* https://nzdotstat.stats.govt.nz/wbos/Index.aspx?DataSetCode=TABLECODE7979. 2022. (Accessed on June 30, 2023)
42) WHO : WHO Coronavirus (COVID-19) Dashboard. https://covid19.who.int/data. 2023. (Accessed on June 30, 2023)
43) OAG : Flight data. https://www.oag.com/. 2021. (Accessed on May 30, 2022)
44) IATA : Air passenger market analysis. https://www.iata.org/en/iata-repository/publications/economic-reports/air-passenger-monthly---dec-2019/. 2019. (Accessed on June 29, 2023)
45) Statista : *Passenger load factor (PLF) on international flights from January 2020 to December 2021, by region.* https://www.statista.com/statistics/234955/passenger-load-factor-plf-on-international-flights/. 2023. (Accessed on June 30, 2023)
46) Wan, R., Zhang, X., & Song, R. : Multi-objective model-based reinforcement learning for infectious disease control. *In Proceedings of the 27th ACM SIGKDD Conference on Knowledge Discovery & Data Mining* (pp. 1634–1644), 2021.
47) Rocha-Filho, C. R., Martins, J. W. L., Lucchetta, R. C., Ramalho, G. S., Trevisani, G. F. M., da Rocha, A. P., Pinto, A. C. P. N., de Assis Reis, F. S., Ferla, L. J., Mastroianni, P. C., Correa, L., Saconato, H., & Trevisani, V. F. M. (2022). Hospitalization costs of coronaviruses diseases in upper-middle-income countries: A systematic review. *PLOS ONE*, 17(3), e0265003, 2022.
48) Adachi, D., Fukai, T., Kawaguchi, D., & Saito, Y. U. : Commuting zones in Japan. *Research Institute of Economy, Trade and Industry (RIETI), 2020*.
49) Australia Bureau of Statistics : Australian Labour Market Statistics. https://www.abs.gov.au/AUSSTATS/abs@.nsf/Previousproducts/6105.0Feature%20Article1Oct%202008. 2008. (Accessed on June 29, 2023)
50) Stats NZ : 2018 Census Main means of travel to work by Statistical Area 2. https://datafinder.stats.govt.nz/table/104720-2018-census-main-means-of-travel-to-work-by-statistical-area-2/. 2018. (Accessed on June 30, 2023)
51) Liu X, Ding Y. : Stability and numerical simulations of a new SVIR model with two delays on COVID-19 booster vaccination. *Mathematics*, 10(10): 1772, 2022.
52) Health New Zealand : *COVID-19 vaccine data.* https://www.tewhatuora.govt.nz/our-health-system/data-and-statistics/covid-vaccine-data. 2023. (Accessed on June 29, 2023)
53) Xin, H., Li, Y., Wu, P., Li, Z., Lau, E. H., Qin, Y., Wang, L., Cowling, B. J., Tsang, T., & Li, Z. : Estimating the latent period of coronavirus disease 2019 (COVID-19). *Clinical Infectious Diseases*, 74(9), 1678–1681, 2022.
54) Mainichi Japan : *Japan's spending on COVID vaccines, medical care hits $122 bil., could increase.* https://mainichi.jp/english/articles/20220506/p2a/00m/0na/038000c. 2022. (Accessed on June 30, 2023)

55) Statista : Number of beds in public hospitals across Australia between 2019 and 2020, by state and territory. https://www.statista.com/statistics/979295/australia-number-of-public-hospital-beds-by-state/. 2022. (Accessed on June 30, 2023)
56) Wikipedia : List of hospitals in New Zealand. https://en.wikipedia.org/wiki/List_of_hospitals_in_New_Zealand. 2023. (Accessed on June 30, 2023)
57) Sun, X., Wandelt, S., & Zhang, A. : Delayed reaction towards emerging COVID-19 variants of concern: Does history repeat itself? *Transportation Research Part A: Policy and Practice*, 152, 203-215, 2021.

(Received)